JOURNAL OF SPACECRAFT AND ROCKETS
Vol. 47, No. 1, January–February 2010

Effect of Simulated Lunar Dust on the Properties of Thermal Control Surfaces

James R. Gaier* and John Siamidis†
NASA John H. Glenn Research Center at Lewis Field, Cleveland, Ohio 44135
and
Elizabeth M.G. Larkin‡
Case Western Reserve University, Cleveland, Ohio 44106

DOI: 10.2514/1.41785

NASA Johnson Space Center's lunar simulant JSC-1AF has been applied to a white thermal control paint and a second-surface mirror thermal control surfaces on aluminum or composite substrates in a simulated lunar environment. The temperature of these surfaces was monitored as they were heated with a solar simulator and cooled in a 30 K cold box. Thermal modeling was used to determine the absorptivity (α) and emissivity (ε) of the thermal control surfaces in both their clean and dusted states. Then, a known amount of power was applied to the samples while in the cold box and the steady-state temperatures measured. It was found that even a submonolayer of simulated lunar dust can significantly degrade the performance of both white paint and second-surface mirror type radiators under simulated lunar conditions. Contrary to earlier studies, dust was found to affect ε as well as α. Dust lowered the emissivity by as much as 16% in the case of the white thermal control paint and raised it by as much as 11% in the case of the second-surface mirror. The degradation of thermal control surface by dust as measured by α/ε rose monotonically regardless of the thermal control coating or substrate, and extrapolated to degradation by a factor 3 at full coverage by dust. Submonolayer coatings of dust were found to not significantly change the steady-state temperature at which a shadowed thermal control surface will radiate.

Nomenclature

f_{dust}	=	Fractional dust coverage (unitless)
α	=	Solar absorptivity (unitless)
α_{rel}	=	Relative absorptivity = (αdusted surface)/(αpristine surface)
ε	=	Thermal emissivity (unitless)
ε_{rel}	=	Relative emissitivty = (εdusted surface)/(εpristine surface)

Introduction

DURING the highly successful Apollo program to land humans on the moon and return them safely to Earth, lunar surface operations were hampered by the effects of a fine, pervasive, highly adhesive dust. The mission records contain references to challenges involving obscuration of vision, clogging of equipment, coating of surfaces, abrasion of surfaces, degradation of seal performance, degradation of thermal performance, and minor health issues. [1] Some of the potentially most serious consequences were due to lunar dust on thermal control surfaces, which caused overheating in several of the science experiments and the batteries of the lunar roving vehicle [2].

The Vision for Space Exploration, announced in 2004, has since been formalized by Congressional legislation as the revised U.S. Space Policy. It calls for a return to the moon by 2020. The current architecture calls for the establishment of a lunar outpost within the first few years which will be inhabited for tours of duty as long as six months. Infrastructure such as power systems and lunar rovers will be expected to have even longer service lives so they can be used by successive crews. Given the extent of the problems caused by dust during the Apollo program, in which the astronauts spent no more than three days on the surface and none of the equipment was reused, it is prudent to try to better understand and mitigate the risk posed by the dust. The objective of this research was to quantify the effects that a submonolayer of lunar dust may be expected to have on thermal control surfaces. It is thought that thick dust layers will be relatively easy to remove from thermal control surfaces by techniques such as brushing, blowing off with a gas jet, or electrostatic removal. It is anticipated, though, that those techniques will not be completely effective and there is a question as to how important it will be to remove what quantity of dust. A second, implied, objective is to establish test protocols for the exposure and characterization of test samples so that the effectiveness of dust mitigation strategies can be quantified. This will be critical for cost-benefit analyses and trade studies.

Methods and Materials

This study used a white thermal control paint (AZ-93) and a second surface mirror silver (Ag) coated FEP Teflon® (AgFEP) as the thermal control surfaces. The thermal control surfaces were applied either to 2.54 cm (1 in.) diameter aluminum substrates, or to identically fabricated composite samples. The composites, which were fabricated inhouse, contained a surface layer of K-1100 high thermal conductivity graphite fibers (Cytec Industries, Inc., West Patterson, NJ) and enough layers of polyacrylonitrile (PAN)-based structural carbon fibers to give a thickness of 6.4 mm (0.25 in.) in a matrix of RS-3 isocyanate resin (YLA, Inc., Benicia, CA). The laminate was laid up as a single sheet and then the round disks were machined from that sheet. The AZ-93 paint was applied by AZ Technology (Huntsville, AL). The AgFEP appliqués were fabricated by Sheldahl, (Northfield, MN) from 12.7 μm (5 mil) thick FEP Teflon® which was coated with a few tens of nm of silver and a few tens of nm of Inconel® as a sealing layer to prevent oxidation. They were hand applied to the samples using adhesive.

The tests were carried out using the NASA lunar dust adhesion bell jar (LDAB). The lunar simulation facility enables the simulated lunar dust to be heated, dried, plasma-cleaned, chemically reduced, and sieved onto samples in situ. It operates at a pressure of 10^{-5} Pa

Received 24 October 2008; revision received 6 July 2009; accepted for publication 21 October 2009.

*Senior Research Scientist, Space Environment and Experiments Branch.
†Aerospace Engineer, Thermal Systems Branch.
‡Adjunct Faculty, Department of Public Health, Medical School.

(10^{-8} torr). The sample, pristine or dusted, can be heated using a 20-sun xenon arc lamp solar simulator, and radiatively cooled in a 30 K cold-box. Details of the LDAB are available elsewhere [3]. Figure 1a shows a photograph of one of the AZ-93 painted composite samples. Two samples of the same material were exposed during each test in a single sample holder. Figure 1b shows two samples mounted in the LDAB samples holder.

One sample was used in the dynamic test where the sample was heated using an unfiltered xenon arc lamp, and then cooled by sliding into a cold-box, which is lined with an absorbing material (Vel-Black®) and maintained at about 30 K with a recycling helium refrigerator. The second sample was used in the steady-state tests and was identical to the first except that a 10Ω resistance heater was bolted to the underside of the sample. The sample was translated into the cold-box and allowed to cool to equilibrium. Then 0.250 W of electrical power was supplied to the heater and the sample allowed to come to a new equilibrium temperature. Subsequently, 1.00 W of electrical power was applied and the sample again allowed to come to its new equilibrium temperature. To minimize heat losses, the samples were supported at their edges by three layers of 0.25 mm (10 mil) thick Kapton®. Temperatures were monitored throughout the test with Type K thermocouples made with 36 American Wire Gauge wire.

The lunar dust simulant chosen for these tests was JSC-1AF. The "F" in the label indicates that it was enriched in the fine fraction, so about half of the particles were 20 μm or smaller. This was the baseline lunar simulant most widely usedby NASA and the community. In bulk chemistry, it closely resembles soils of the lunar mare that were returned during Apollo 14. It was selected, not because it is the best simulant available but because it was the de facto NASA standard.

Lunar simulant dust was loaded into a bowl within the LDAB where it was conditioned so that it might be more lunar like. The chamber was pumped to a vacuum of 10^1 Pa (10^{-1} torr) using a mechanical roughing pump while intermittently stirring the dust. Then a radio frequency air plasma was ignited which generated oxygen ions and ultraviolet light which cleaned organic contaminants off of the dust for at least 1 h. The lunar simulant was degassed in vacuum at high temperature ($>200^{\circ}C$) overnight with intermittent stirring. It was then subjected to a 4% hydrogen in helium plasma for 1 h to chemically reduce the surface and implant some amount of hydrogen into the dust grains, to simulate the implanted solar wind on the lunar surface. The dust was applied to the samples through either a 25 or a 32 μm sieve so that only the fine particle fraction would be applied. Submonolayer coatings of dust (the surface is not completely coated by even a thin a layer of dust) were applied in all cases for these tests.

It proved surprisingly difficult to apply an even coating of dust on thermal control surface samples. It was thought that a simple sinusoidal motion of the sieve would deposit the dust evenly and reproducibly. This proved not to be the case. Varieties of jarring and vibrating motions were also employed but did not give consistently even coatings. The treated dust did not behave in vacuo the same way it did in air, so test runs in an open vacuum chamber were of limited utility. The dust application pattern also varied over time and was not reproducible. Time that the dust was sifted onto the sample correlated very poorly with the amount of dust deposited. That is, more dust may be deposited in a 60 s run than on a subsequent 600 s run. Typical results are shown in Fig. 2. It can be readily seen that the left sample, particularly on its left half, has much more dust deposited on it than the right sample.

The characterization of f_{dust} was complicated by the fact that all particles deposited on the samples were smaller than 32 μm because of the sieve. Thus, although the right hand sample in Fig. 2 appears to be clean, microscopic investigation revealed that about 5% of its surface was covered with dust and indeed its α is increased.

Determining the f_{dust} on the thermal control surface by a submonolayer of sub-25 μm particles was not straightforward. To count such small particles, magnification of at least 100× is required. The dust appears dark on the AZ-93 coating, but light on the AgFEP coatings, as can be seen in Fig. 3. At 100× the area imaged by our microscope was 968 × 726 μm, so there were 641 nonoverlapping frames on the sample disk. Rather than count the particles in all 641 frames for each of 17 samples (nearly 11,000 photos) it was decided to analyze a statistically significant random sample of the frames. A 95% confidence interval (CI) was also calculated around each mean to determine the precision of this estimated mean. Details of the analysis procedure have been published elsewhere [4].

The thermal modeling was done using Thermal Desktop (Cullimore & Ring Technologies), a PC based design environment for generating thermal models of electronics and vehicles. Thermal Desktop incorporated both parameter based finite-difference surfaces with finite elements and CAD technology to model thermal problems. Thermal Desktop developed the capacitance and conductance network for input to SINDA/FLUINT which was a comprehensive finite-difference, lumped parameter (circuit or network analogy) tool for heat transfer design analysis and fluid flow analysis in complex systems. Thermal Desktop 5.1 Patch 3 was used to generate the thermal model, which consists of 743 nodes and 1840 linear conductors. A visualization of the model and the material parameters used in it are shown in Fig. 4.

For the pristine samples during heating, the optical properties (α and ε) of the coated sample were set to the initial values. Subsequently, the power of the heating lamp was varied to match the temperature of the test run. Once the power of the lamp was established, the α was varied for each test run until there was less than 1.0% difference in the weighted average temperatures between each test run and the corresponding analysis run. During cooling, the ε was

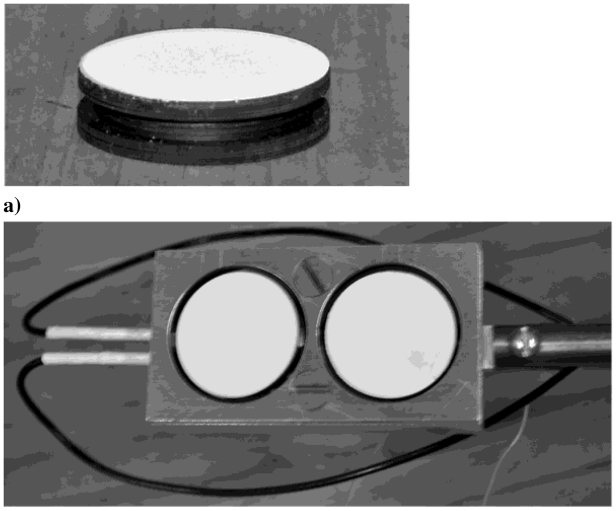

a)

b)

Fig. 1 a) Composite sample coated with AZ-93, b) two 2.54 cm diameter samples of AZ-93 coated aluminum in the sample holder.

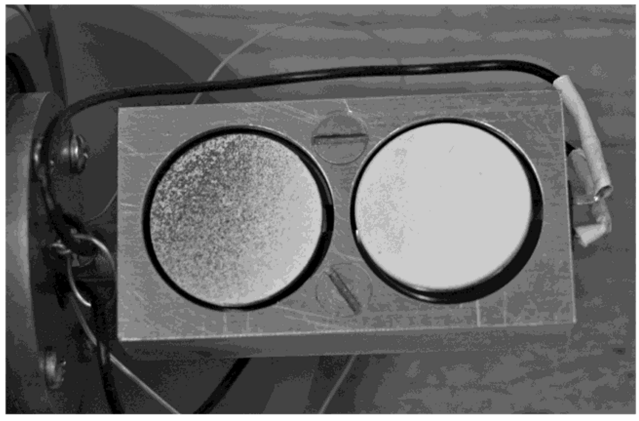

Fig. 2 Photograph of the two samples, number AZ93Al-1, that were dusted at the same time in the configuration shown.

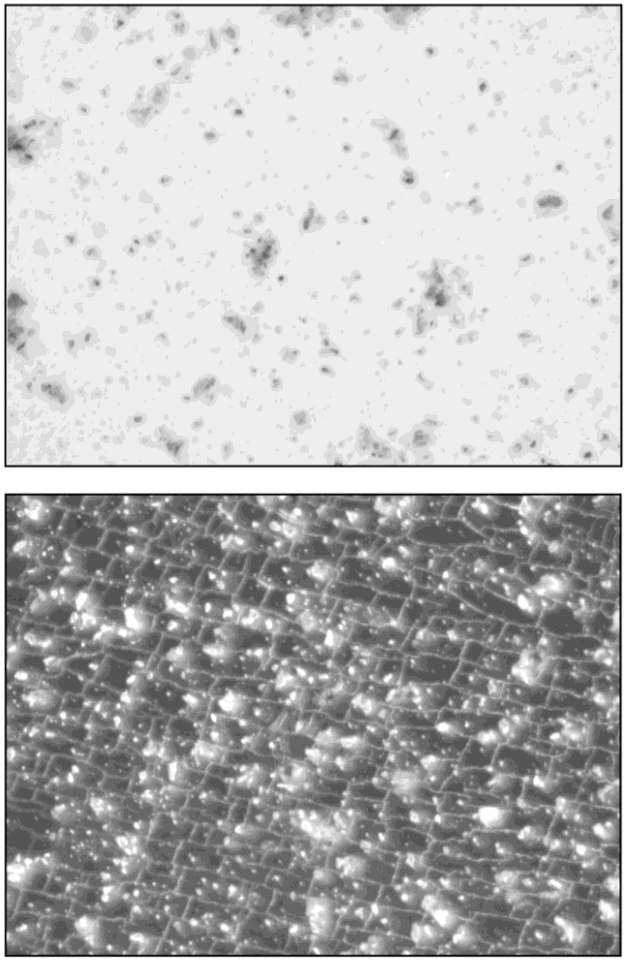

Fig. 3 Photomicrographs of the AZ-93 sample (top) and AgFEP sample (bottom) that were used in the analysis of f_{dust}. The area covered in each photomicrograph is about 1 mm^2.

varied for each test run until there was less than 1.0% difference in the weighted average temperatures between each test and analysis run.

For the dusted samples during heating, the α was varied for each test run using the previously determined lamp power until there was less than 1.0% difference in the weighted average temperatures between each test and analysis run. During cooling, the ε was varied for each test run until there was less than 1.0% difference in the weighted average temperatures between each test and analysis run.

Dynamic Test Results on Pristine Samples

To determine the quality of data generated by the LDAB, two sets of dynamic test measurements (heating and cooling) were made on the same pristine AZ-93 consecutively without the addition of dust. The heating and cooling curves are shown in Fig. 5. They show that the instrument reproducibility of the LDAB calorimetry system is good. The thermal optical properties determined from the model fit to the heating and cooling curves of the samples are summarized in Table 1 and discussed below.

The heating and cooling curves from AZ-93 painted aluminum were measured on four samples, one of which was measured twice (as shown in Fig. 5). The mean α of the coatings was found to be 0.173 with a standard deviation of 0.029, and the model fit the data to within 0.03% in all five cases. The ε was measured to be 0.886 ± 0.024, with the model fit to the data being within 1.7%. It should be pointed out that variations in lamp intensity, translational and rotational sample positioning, and errors in the temperature dependence of thermal properties are all swept into α and ε by the model. Nevertheless, the values determined for α and ε are within the range of literature values for the variation in AZ-93.

The heating and cooling curves from AZ-93 painted composite samples were also measured on four samples. The α of the coating was found to be 0.196 ± 0.006, with the model fitting the data within 0.06% or less in all four cases. The ε was 0.833 ± 0.027, with the model fitting the data within 0.28%. The values determined for α were within the expected values, but the ε values were a bit low. In comparing α and ε of the same paint applied to the two different surfaces, it is noted that the α is somewhat higher (13%) for the composite samples and the ε is somewhat lower (6% lower). The higher α of the painted composite could be explained if the paint is not entirely opaque, since the alpha of the composite is much higher than that of the aluminum.

The heating and cooling curves for AgFEP adhered to aluminum substrates were measured for seven trials on four different samples. As with the AZ-93 samples the reproducibility of the experiment was quite good. The α of the coating was found to be 0.073 ± 0.006, with the model fit of the data within 0.10% in all seven cases. The ε was 0.719 ± 0.041, and the model fit within 0.46%. The values determined for α are well within the literature values for AgFEP, but once again the ε values were somewhat low.

The heating and cooling curves for AgFEP adhered to composite substrates for five different samples were also measured. The reproducibility of the experiment was not quite as good as the other experiments. The α of the coating was found to be 0.101 ± 0.025, and the ε was 0.648 ± 0.038. In spite of this spread the α model fit the data within 0.09% or better in all four cases, and the ε model within 1.31%. Although the values determined for α are well within the literature norms, the ε was pretty low compared with the literature values for AgFEP.

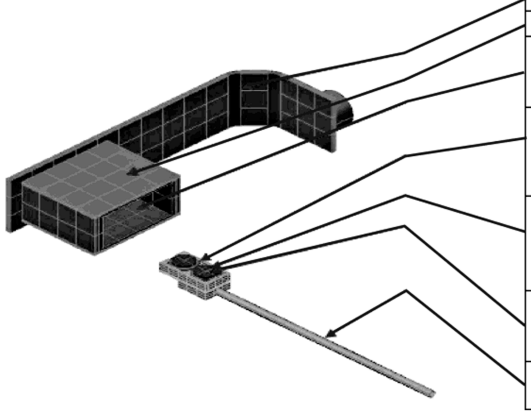

	Material	Material cond., W/mK	Material cp., J/KgK	Material finish	Material finish α/ε
Chamber	SS 316	16.3	504	SS polished	0.42/0.11
Blend copper	Copper	406.4	380	Buffed copper	0.30/0.03
Copper box	Copper	406.4	380	Buffed copper	0.30/0.03
Vel-black layer inside copper box	Carbon fiber	360	628	Black paint	0.95/0.95
Sample holder	AL 6061-T8	f(T) = 43.3 at 32 K to 175.6 at 743.9K	f(T) = 64.6 at 34.6 K to 1126.8 at 810.9K	Al polished	0.15/0.05
Aluminum sample	AL 6061-T8	f(T) = 43.3 at 32 K to 175.6 at 743.9K	f(T) = 64.6 at 34.6 K to 1126.8 at 810.9K	Z-93	Initial 0.20/0.91 then varied
Composite sample	3 layer composite	Varies by layer 1st layer; 1100 2nd and 3rd; 5	~1000	AgFEP	Initial 0.08/0.81 then varied
Sample holder rod	SS 304	16.3	500	SS machined	0.47/0.14

Fig. 4 Picture of the thermal model and parameters used in its construction.

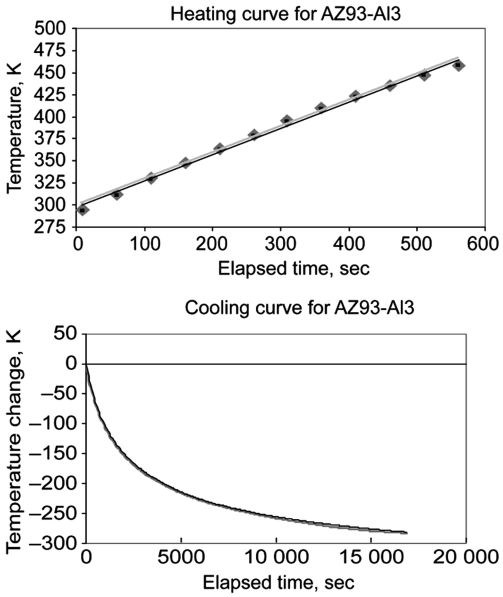

Fig. 5 Heating curve and cooling curve for sample number AZ93Al-3 taken two different days (◆) and (■).

One measure of this type of thermal control surface is its α/ε ratio, with the best thermal control surfaces having a small value. This is shown in the last column of Table 1. The AZ-93 painted on aluminum has an α/ε of 0.195, very close to the literature value. The composite α/ε, however, is more than 20% higher. It is suspected that most of the literature values come from samples painted on low α surfaces, like aluminum, and this may account for at least some of the difference. The α/ε for the AgFEP samples widely bracketed the literature values. It is again noted that the AgFEP delaminated from many of the composite samples, which probably distorts the value. But an overall look at Table 1 reveals that all of the values, both α and ε, except for the AZ-93 on composite α are lower than the reported literature values. This may reflect the sweeping of all other variations and errors into the α and ε values, as noted earlier.

Dynamic Test Results on Dusted Samples

Dust obscured the four AZ-93 painted aluminum surfaces with f_{dust} of 0.13, 0.50, 0.50, and 0.53. Although a wider spread of f_{dust} would be desirable, it was not possible to experimentally determine how much dust had been deposited in situ. The horizontal lines bound the 95% confidence interval resulting from the measurement of the f_{dust} coverage in 50 randomly chosen frames [4]. The α_{rel} as a function of percent coverage is shown as the open diamonds in Fig. 6. The model fit the α data to 0.05% or better. Note that the more heavily a sample is covered with dust, the higher the α. This is what would be expected by putting dark dust on a white paint.

Dust obscured the four AZ-93 painted composite surfaces with f_{dust} of 0.16, 0.24, 0.54, and 0.55. The α_{rel} as a function of f_{dust} is shown as the filled diamonds in Fig. 6. The horizontal lines bound the 95% confidence interval resulting from the measurement of the f_{dust} in 50 frames. The model fit the α data to 0.15% or better. Note that the α was somewhat lower than it was on the aluminum substrates. This may be the result of the paint layer not being totally opaque since the α of the composite substrate is much higher than that of the aluminum.

Table 1 Thermal optical properties of pristine thermal control surfaces

Pristine material	Emissivity (ε)	Absorptivity (α)	α/ε
Literature AZ–93	0.910 ± 0.010	0.175 ± 0.025	0.192
AZ–93 on Al	0.886 ± 0.024	0.173 ± 0.029	0.195
AZ–93 on composite	0.833 ± 0.027	0.196 ± 0.006	0.235
Literature AgFEP	0.810 ± 0.010	0.105 ± 0.025	0.130
AgFEP on Al	0.719 ± 0.041	0.073 ± 0.006	0.102
AgFEP on composite	0.648 ± 0.038	0.101 ± 0.025	0.156

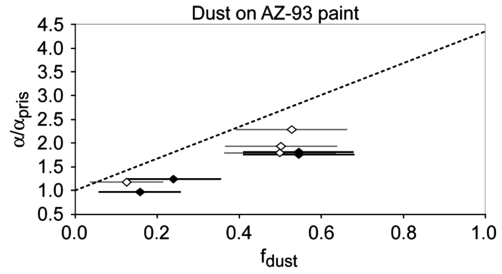

Fig. 6 Plot of $\alpha/\alpha_{\text{pris}}$ as a function of f_{dust} for the AZ-93 painted aluminum (◇), composite (◆), and the rule of mixtures (——).

At this point a comparison can be made between the measured α and that which might be expected. A reasonable model to use is the rule of mixtures model which states that there are no interactions between the dust particles and the thermal control surface. Thus, if a surface is one-quarter covered with dust, the α of that one-quarter should have the α of bulk dust, and the α of the remaining three-quarters of the surface should be unaffected. The definition of α_{rel} can be written in terms of the rule of mixtures as Eq. (1):

$$\alpha_{\text{rel}} = \frac{(f_{\text{dust}}\alpha_{\text{dust}} + (1 - f_{\text{dust}})\alpha_{\text{pris}})}{\alpha_{\text{pris}}} \tag{1}$$

From the literature, the α_{dust} is taken to be 0.76, and the α_{pris} is taken to be 0.175 for AZ-93. Figure 6 shows the rule of mixtures results as a dotted line.

The measured values of α fall considerably below the rule of mixtures line. The discrepancy appears too systematic for it to be a result of experimental errors in either the f_{dust} measurements or the α measurements. It is possible that the α is lower because the bulk value for the lunar regolith α was used. As can be seen in Fig. 7, most of the individual grains of the JSC-1AF lunar simulant are transparent (being plagioclase). So perhaps part of the light that gets trapped in multiple layers of dust is simply transmitted through to the coating when it is submonolayer.

It has been the conventional wisdom that since the lunar regolith is so dark that dust on a thermal control surface will have no appreciable effect on the ε. The data plotted in Fig. 8, however, suggest that there may be a drop off in the ε of AZ-93 even as less than a monolayer of dust accumulates on it. The model fit the ε data to 0.42% or better for the AZ-93 on aluminum and 0.28% or better for the composite substrate. When fully covered, ε may well drop to a level that is less than 80% that of clean AZ-93, which may bring it below 0.70. This is significant degradation.

Dust obscured the four AgFEP applied to aluminum surfaces with f_{dust} of 0.13, 0.13, 0.21, and 0.48. The α_{rel} as a function of f_{dust} is shown as the open diamonds in Fig. 9. The horizontal lines bound the 95% confidence interval resulting from the measurement of f_{dust} in 50 frames. The model fit the α data to 0.30% or better. Note again that the more heavily a sample is covered with dust, the higher the α. This is what would be expected by putting dark dust on a reflective surface.

Dust obscured the four AgFEP applied to composite surfaces with f_{dust} of 0.05, 0.35, 0.36, and 0.39. There were problems with the composite outgassing and bubbles being trapped under the FEP, causing it to pull away from the substrate in places. Not only does this affect the heat transfer properties between the FEP and the substrate, but it also made the f_{dust} determination difficult because many of the frames were not flat enough for the microscope to focus well on. Since the dust coverage is determined optically, this throws an additional source of error into f_{dust}. For these samples the α_{rel} as a function of f_{dust} is shown as the filled diamonds in Fig. 9. The horizontal lines bound the 95% confidence interval resulting from the measurement of f_{dust} in 50 frames. The model fit the α data to 0.15% or better.

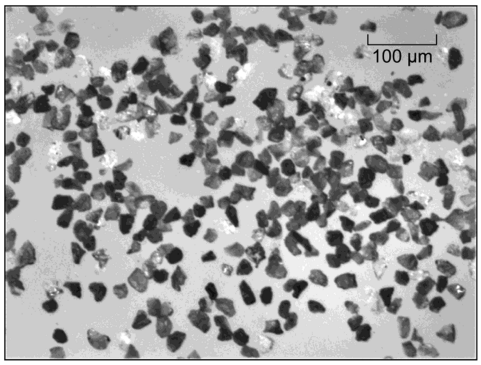

Fig. 7 Photomicrograph of JSC-1AF lunar simulant.

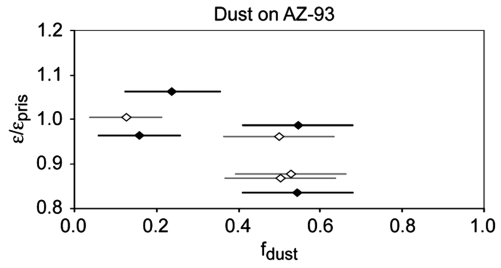

Fig. 8 Plot of $\varepsilon/\varepsilon_{\text{pris}}$ as a function of f_{dust} for the AZ-93 painted on aluminum (◇) and composite (◆) substrates.

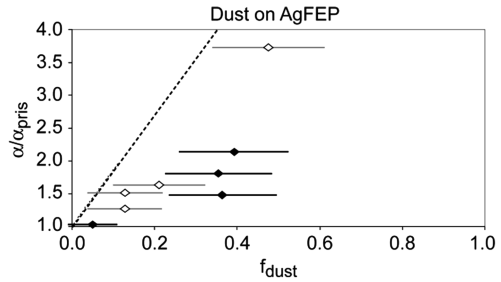

Fig. 9 Plot of $\alpha/\alpha_{\text{pris}}$ as a function of f_{dust} coverage for the AgFEP applied to aluminum (◇), composite (◆), and the rule of mixtures (——).

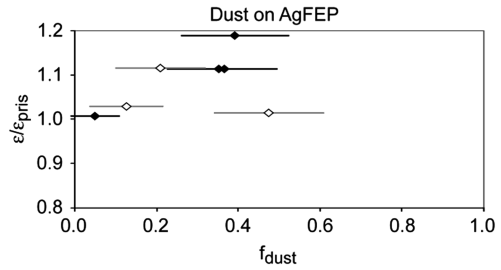

Fig. 10 Plot of $\varepsilon/\varepsilon_{\text{pris}}$ as a function of f_{dust} for the AgFEP on aluminum (◇) and composite (◆) substrates.

The comparison between the measured α increases due to dust deposition and those which might be expected using the rule of mixtures (dotted line) is also shown in Fig. 9. Once again the data, even including the range represented by the 95% confidence interval, fall considerably below the rule of mixtures model line. Even though the effect of dust on AgFEP is predicted to be more severe than on AZ-93 samples, the relationship between the rule of mixtures model and the measured data is similar.

Given the effect of dust on the ε of AZ-93 shown in Fig. 8, it is perhaps surprising that dust on AgFEP appears to have the opposite effect. Figure 10 shows that ε increases with dust coverage. When fully covered, ε may well rise to a level as high as 1.3 times greater than that of clean AgFEP, which may raise it above 0.90. This is a significant enhancement.

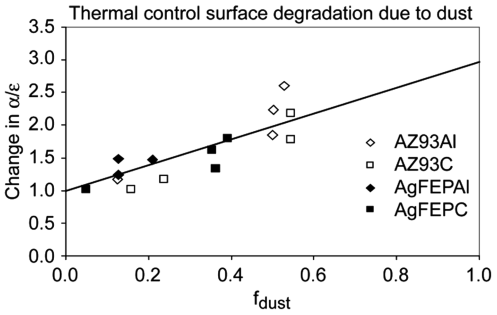

Fig. 11 The total change in α/ε as a function of f_{dust}.

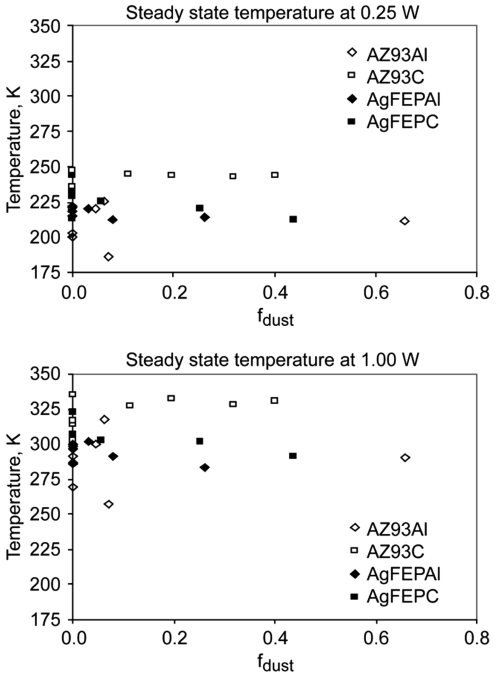

Fig. 12 The steady-state temperatures of pristine and dusted samples radiating to a 30 K background with 0.25 and 1.00 W applied power.

To judge the overall thermal performance of a thermal control surface both the α and ε of the surface must be accounted for, generally as the ratio α/ε. Figure 11 is a plot of the total change in α/ε as a function of dust coverage for each of the four types of samples measured in this study. Interestingly, the α/ε values rose monotonically with dust coverage regardless of the thermal control coating or substrate. A least squares line had an R^2 of 0.72, and extrapolated to degradation by a factor 3 for full coverage by dust.

Steady-State Test Results

The results of the steady-state temperature when 0.25 or 1.00 W was applied to the sample while in a 30 K cold-box are illustrated in Fig. 12. Two trends are apparent from these plots. First, it appears that the spread in the steady-state temperatures of the pristine samples was as wide as the span of dust covered temperatures. This implies a submonolayer level of dust coverage would not cause a shaded radiator to run hotter. Second, it appears that the AgFEP aluminum samples ran significantly (30 to 35 K) hotter than the other samples, and this was most evident when they had dust on them. The AgFEP composite radiator samples ran somewhat hotter than the AZ-93, particularly when clean. The AZ-93 on aluminum radiators ran the coolest.

Conclusions

There are three major conclusions that can be drawn from this study. The first is that even a submonolayer of simulated lunar dust can significantly degrade the performance of both white paint and second-surface mirror type radiators under simulated lunar conditions. As little as 12% dust coverage can degrade the α by as much as 50%.

The second conclusion is that the dust has an effect on the ε as well. It degrades it by as much as 16% in the case of 54% covered AZ-93 and improves it by as much as 11% in the case of 35% covered AgFEP. The degradation of thermal control surfaces by dust as measured by α/ε seems to rise monotonically, regardless of the thermal control coating or substrate, and is extrapolated to degradation by a factor 3 at full coverage by dust.

The third conclusion is that submonolayer coatings of dust do not significantly change the steady-state temperature at which a shadowed thermal control surface will radiate. This again emphasizes that although the ε is altered by the presence of a submonolayer dust, the change in α is the major effect, and in the absence of incident radiation the dust has little effect on radiator performance.

Acknowledgments

This work is the result of a great deal of effort by a sizable team of dedicated professionals from many organizations. In addition to the authors, Scott R. Panko (Arctic Slope Research Corporation), Edward A. Sechkar (Arctic Slope Research Corporation), and Frank P. Lam (Sierra Lobo Test Facilities, Operations, Maintenance, & Engineering) provided test, engineering, and technical support of the lunar dust adhesion bell jar facility. Donald A. Jaworske (NASA John H. Glenn Research Center at Lewis Field) oversaw the fabrication of the test samples and acted as a general resource on thermal control coatings. Mark J. Hyatt (NASA John H. Glenn Research Center at Lewis Field) and Ryan Stephan (NASA Johnson Space Center) provided continued program guidance. Kerry J. Rogers (Lewis Educational Research and Collaboration Internship Program student, Manchester College, North Manchester, Indiana) provided much of the actual particle counting for the dust coverage measurements.

References

[1] Gaier, J. R., "The Effects of Lunar Dust on EVA Systems During the Apollo Missions," NASA TM-2005-213610/REV1, 2007.

[2] Gaier, J. R., and Jaworske, D. A., "Lunar Dust on Heat Rejection System Surfaces: Problems and Prospects," NASA, Rept. TM-2007-214814, 2007.

[3] Gaier, J. R., and Sechkar, E. A., "Lunar Simulation in the Lunar Dust Adhesion Bell Jar," AIAA Paper 2007-0963, 2007;also NASA TM-2007-214704, 2007.

[4] Gaier, J. R., Siamidis, J., and Larkin, E. M. G., "Extraction of Thermal Performance Values from Samples in the Lunar Dust Adhesion Bell Jar," NASA, Rept. CP-2008-214164, 2008.

J. Minow
Associate Editor